Proceedings of the 11th International Conference of Control Systems, and Robotics (CDSR 2024)
Chestnut Conference Centre - University of Toronto, Toronto, Canada – 10 -12 June, 2024
Paper No. 138
DOI: 10.11159/cdsr24.138

Design and Control of the Omnidirectional Robot for Floor Polishing Tasks

Javier Vega-Gutiérrez[1], Mario Ramírez-Neria[1], Rodrigo Ramírez-Juárez[1], Axel Becerril-Velasco[1], Alejandro Martínez Valdez[1]
[1]INIAT Institute of Applied Research and Technology, Universidad Iberoamericana Ciudad de México
Prolongación Paseo de la Reforma 880, Colonia Lomas de Santa Fe, CP 01219, México
A2281283@correo.uia.mx; mario.ramirez@ibero.mx
juarezrgo@gmail.com

Abstract – This paper explores the design and control of an omnidirectional robot for polishing tasks, addressing challenges in traditional machines' operation. A prototype system with advanced control mechanisms, including a 1.5 hp motor and four actuators, is designed and evaluated. The system demonstrates good results at controlling velocity wheels and robot orientation, rejecting torsional forces provided by the cleaning disc when it is rotating; this robot could contribute to efficiency and safety in cleaning tasks.

Keywords: Omni-directional robot, Service robot, Polishing Process, Kinematic modeling

1. Introduction

In recent years, advancements in mobile robotics have led to the development of omnidirectional robots, particularly in cleaning tasks such as floor polishing prevalent in Mexico. Traditional polishing machines pose challenges due to their operational dynamics, requiring skilled operators to mitigate movements and control forces.

This research aims to address these challenges by designing and evaluating a prototype floor polishing system with advanced control mechanisms. The prototype integrates a 1.5 hp motor and four actuators to counteract dynamic effects, alongside kinematic modeling and visual evidence of remote control, obstacle detection, and autonomous system action.

This paper presents the results of the design process and evaluation of the prototype, offering insights into its functionality and potential applications in enhancing floor polishing processes.

2. Problem statement

The project addresses the complexity of polishing machines in the cleaning sector, where high turnover rates lead to inexperienced operators potentially damaging surfaces.

At Universidad Iberoamericana, the Vicon Motion system was used to quantitatively assess operator Experience. Two tests compared the movements of experienced and inexperienced operators, highlighting differences in trajectories (see Figure 1).

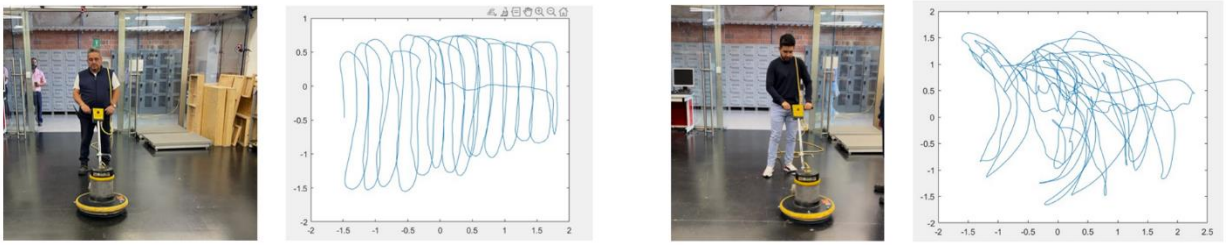

Figure 1 Difference between polishing patterns of an experienced operator and an inexperienced one.

3. Traction Control and Trajectory Tracking

The kinematic model of the equipment, depicted with wheels as shown in Figure 2, is derived as follows. An inertial frame G = [XG, YG, ZG] is considered, where [x, y] denote the position of the robot's center of mass relative to frame G, and ϕ represents its orientation with respect to XG [1] [2]. Additionally, a coordinate frame B = [XB, YB, ZB] is attached to the robot's center of mass, where ω represents its angular velocity, and VX and VY denote its linear velocities with respect to the XB and YB axes, respectively [3]-[5].

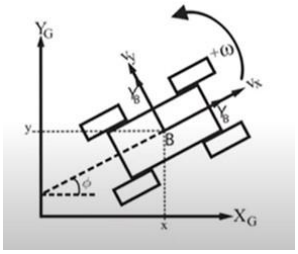

Figure 2 Representation of an omnidirectional robot in the G framework

Then, the coordinates of the robot's center of mass are defined as $[x_c, y_c]$, and ϕ as its angular orientation concerning to the XG axis. The objective of formulating the model is to relate the robot's velocities with the velocities of the tires defined as $V_x, V_y \; and \; \omega$. Therefore, we establish $\dot{x}$ and $\dot{y}$ as:

$$\dot{x} = \dot{x_c} = V_x Cos(\phi) - V_y Sin(\phi) \quad (1)$$

$$\dot{y} = \dot{y_c} = V_x Sin(\phi) + V_y Cos(\phi) \quad (2)$$

$$\dot{\phi} = \omega \quad (3)$$

The next step is to find a relationship between the robot velocities $V_x, V_y \; and \; \omega$ and the velocities of each wheel, denoted as $\omega_1, \omega_2, \omega_3$ y ω_4. For this purpose, we analyze the distribution of the wheels shown in figure 3 [6] [7].

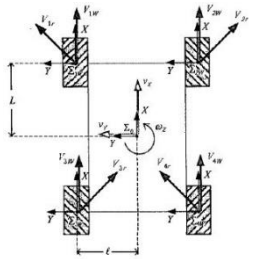

Figure 3 Distribution of Mecanum wheels in an omnidirectional robot

Next, V_{iew} represents the tangential velocity at each wheel, given by $V_{iw} = \omega iw$, where ωiw is the wheel's angular velocity, and R_w is its radius. V_{ir} denotes the tangential velocity of the roller in contact with the floor at each wheel.

Subsequently, an analysis of velocities concerning the X and Y axes is performed. V_{ix} is the sum of the tangential velocity and the velocity contributed by the rollers, while V_{iy} comprises only the component contributed by the tangential velocity of the rollers.

After implicating the equations, we obtain the expression that represents the inverse kinematic problem, that is, obtaining the angular velocities as a function of the linear and angular velocities of the robot.

$$V_w = JV_0 \tag{8}$$

Where $V_0 = \left[v_x\ v_y\ w_z\right]^T$ is the vector of the linear and angular velocities of the robot, I is the identity matrix, while while $V_w = [w_1\ w_2\ w_3\ w_4]^T$ is the vector of wheel velocities, i.e., the angular velocity of the wheels [8] [9]. Therefore, J must be a transformation matrix defined as

$$J = \begin{bmatrix} 1 & 1 & -(L+l) \\ 1 & -1 & (L+l) \\ 1 & -1 & -(L+l) \\ 1 & 1 & (L+l) \end{bmatrix} \tag{9}$$

On the other hand, the linear velocities of the equipment can be obtained from the angular velocities of each wheel, but to do so, the pseudo-inverse matrix J+J+ is required, such that:

$$V_0 = J^+ V_w + (I - J^+)\omega^* \tag{10}$$

Where $J^+ = (J^T J)^{-1} J^T$, ω^* can be taken arbitrarily, and since R_w is the radius of the wheels, the forward kinematics equations for $\omega^* = 0$ are:

$$\begin{bmatrix} v_x \\ v_y \\ w_z \end{bmatrix} = \begin{bmatrix} \frac{1}{4} & \frac{1}{4} & \frac{1}{4} & \frac{1}{4} \\ \frac{-1}{4} & \frac{1}{4} & \frac{1}{4} & \frac{-1}{4} \\ \frac{-1}{(L+l)} & \frac{1}{(L+l)} & \frac{1}{(L+l)} & \frac{-1}{(L+l)} \end{bmatrix} \begin{bmatrix} R_w\dot{\theta}_1 \\ R_w\dot{\theta}_2 \\ R_w\dot{\theta}_3 \\ R_w\dot{\theta}_4 \end{bmatrix} \tag{11}$$

Finally, the expressions for the linear velocities in x, y and ω of the robot are given by:

$$v_x = \frac{R_w}{4}\left(\dot{\theta}_1 + \dot{\theta}_2 + \dot{\theta}_3 + \dot{\theta}_4\right) \tag{20}$$

$$v_y = \frac{R_w}{4}\left(-\dot{\theta}_1 + \dot{\theta}_2 + \dot{\theta}_3 - \dot{\theta}_4\right) \tag{21}$$

$$w_z = \frac{R_w}{4(L+l)}\left(-\dot{\theta}_1 + \dot{\theta}_2 - \dot{\theta}_3 + \dot{\theta}_4\right) \tag{22}$$

4. Experimental Implementation

The developed prototype features remote manipulation functions, obstacle detection, and inhibition of internal and external disturbances with the purpose of providing greater safety and autonomy to the polishing process. To achieve this, components that are not part of commercial equipment were added, which are listed below:

Table 1 Bill of materials to increase the level of automation of the system.

Sub-system	Traction System	Quantity
Power Supply	12V 50A Power Supply	1
	SSR-40 DA Solid-State Relay	1
	H-Bridge HBTN7960	4
	Yellow Jacket Planetary Gear Motor (50.9:1) Series 5202	4

Traction	Set of 4 Mecanum Wheels with 45 Kg Capacity (Each with a load capacity of 50Kg)	1
	16mm Bushings	4
Control	STM32E4 DISCOVERY	1
	ESP32 38-pin ESP WROOM 32	2
Structural	Nylamid Board Type -M- 12.7 x 610 x 610 mm	1
	1 kg of PLA Filament for 3D Printer	1
	1202 Series Angle Pattern Mount (1-3)	4

For the implementation of the control system to perform torque rejection generated by the cleaning disk, Waijung 15 was used to load the control blocks created in Simulink onto a board (Figure 4).

The board used to control the motor according to the design of the control systems was an STM32. The mapping of the connections made is shown in the Figure 5.

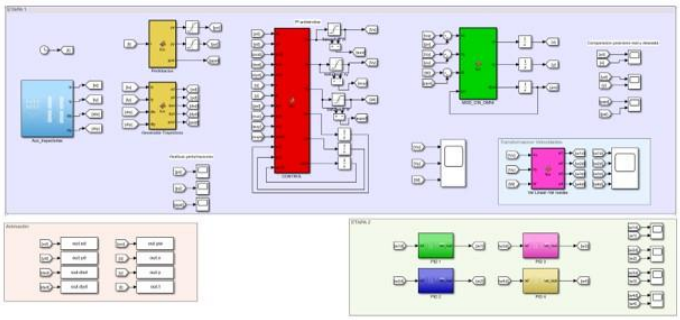

Figure 4 Control scheme developed in Simulink.

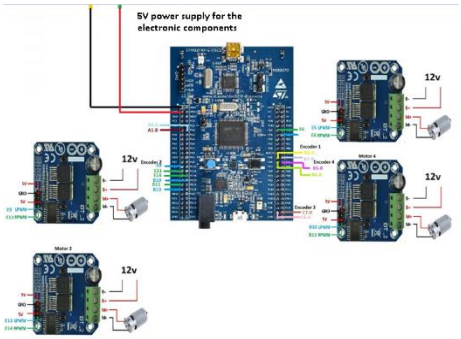

Figure 5 Diagram of connections between the STM32 and the motor H-bridges.

The result of integrating all the components is the implementation of the equipment shown in figure 6.

Figure 6 Result of the system implementation.

5. Experimental results

Since each wheel changes the required speed to ensure that the system always achieves its three main objectives:

Inhibiting the resulting torque that acts as a disturbance in the system, which, as mentioned earlier, in commercial machines is compensated for by the operator. As seen in the following video:

https://www.youtube.com/watch?v=gqGz25lLNhA

On the other hand, in the following link, you can observe the behavior of the equipment when the polisher disk motor is activated, but with the control turned off. Basically, the system is unable to maintain its orientation.

https://www.youtube.com/shorts/W5dQichgoqM

Moreover, the system can handle the application of an external force on the body of the equipment.

https://youtube.com/shorts/wewyKtCRLj0

Follow a uniform trajectory for surface polishing. In the following link, it shows the trajectory control in a teleoperated manner, meaning it does not require physical contact between the operator and the chassis of the equipment. In commercial equipment, the operator simultaneously compensates for system torques.

https://www.youtube.com/shorts/XacU198UFVY

Finally, emergency stop functions are added in case an obstacle is encountered in the equipment's forward direction. The video shows the activation of this safety stop without the need for the operator to stop the equipment manually.

https://www.youtube.com/shorts/jqeXpqI3iHw

6. Conclusion

Commercial polishing machines rely entirely on operator intervention to maintain their trajectory and perform the necessary movements for the procedure. The results obtained from this work demonstrate the implementation of a control system capable of counteracting the rotational disturbance generated by the disk against the floor, with the controller leveraging the reactions between the wheels to generate a torque opposing the disturbance, resulting in a system capable of maintaining its orientation and trajectory while polishing a surface.

Acknowledgements

This work was supported by the Universidad Iberoamericana Ciudad de México, Prolongación Paseo de la Reforma 880, Colonia Lomas de Santa Fe,Álvaro Obregón, Ciudad de México 01219.

References

[1] K.-L. Han, O.-K. Choi, J. Kim, H. Kim and J. Lee, "Design and control of mobile robot with Mecanum wheel," *ICCAS-SICE 2009 - ICROS-SICE International Joint Conference 2009, Proceedings,* pp. 2932 - 2937, 09 2009.

[2] L. Jaulin, Mobile robotics, John Wiley & Sons, 2019.

[3] F. Rubio, F. Valero and C. Llopis-Albert, "A review of mobile robots: Concepts, methods, theoretical framework, and applications," *International Journal of Advanced Robotic Systems,* vol. 16, 2019.

[4] R. Siegwart, I. R. Nourbakhsh and D. Scaramuzza, Introduction to autonomous mobile robots, MIT press, 2011.

[5] F. Becker and O. Bondarev, "An approach to the kinematics and dynamics of a four-wheel Mecanum vehicle," *Sci. J. IFToMM Probl. Mech,* vol. 2, pp. 27--37, 2014.

[6] C. Canuda, Theory of Robot Control, SPRINGER, 1996.

[7] H. Taheri, B. Qiao and N. Ghaeminezhad, "Kinematic model of a four mecanum wheeled mobile robot," *International journal of computer applications,* vol. 113, pp. 6--9, 2015.

[8] I. Doroftei, V. Grosu, V. Spinu and others, Omnidirectional mobile robot-design and implementation, London, UK: INTECH Open Access Publisher, 2007.

[9] E. Saenz and V. Bugarin, "Kinematic and dynamic modeling of a four wheel omnidirectional mobile robot considering actuator dynamics," *AMRob J,* vol. 4, pp. 114--120, 2016.

[10] P. Viboonchaicheep, A. Shimada and Y. Kosaka, "Position rectification control for Mecanum wheeled omni-directional vehicles," in *IECON'03. 29th Annual Conference of the IEEE Industrial Electronics Society (IEEE Cat. No.03CH37468)*.